34th Annual International Conference of the IEEE EMBS
San Diego, California USA, 28 August - 1 September, 2012

Discriminating Multiple Motor Imageries of Human Hands Using EEG*

Ran Xiao, *Student Member, IEEE*, Ke Liao, Lei Ding, *Member, IEEE*

***Abstract*— We investigated the feasibility of discriminating four different motor imagery (MI) types from both hands using electroencephalography (EEG) through exploring underlying features related to MIs of thumb and fist from one hand. New spectral and spatial features related to different MIs were extracted using principal component analysis (PCA) and squared cross correlation (R^2). Extracted features were evaluated using a linear discriminant analysis (LDA) classifier, resulting in an average decoding accuracy about 50%, which is significantly higher than the guess level and the 95% confidence level of guess. The preliminary results demonstrate the great potential of extracting features from different MIs from same hands to generate control signals with more degrees of freedom (DOF) for non-invasive brain-computer interface applications. In addition, for movement related applications, especially for neuroprosthesis, the present study may facilitate the development of a non-invasive BCI, which is highly intuitive and based on users' spontaneous intentions.**

I. Introduction

Noninvasive brain computer interface (BCI) techniques decode electromagnetic signals measured from the human brain, and translate them into control commands for computer programs or external devices [1]. These techniques build an alternative channel between the user's brain and outer environment, bypassing normal motor output pathways [2]. This could be useful for people suffering from severe motor disability to regain communication and control in daily life [3], [4].

The field of BCI research is growing rapidly with advancements in biomedical devices and signal processing techniques. Various neurophysiological patterns have been identified and utilized as control features for BCI systems, including mu rhythms induced in motor imagery (MI) [5], event-related P300 [6], steady state visual evoked potentials (SSVEP) [7], and many others. Among them, MI related patterns have been widely used in movement related applications, such as cursor task [2], [8].

While various MI-based BCIs have been developed, one remaining challenge is the limited number of features available to produce enough control signals, which largely defines the complexity of applications. Recent studies implemented MI from hands and other body parts to generate control signals with three degrees of freedom (DOFs) to move a cursor on computer screens [8]. However, for applications with more complexities, such as neuroprosthesis, it is far from enough. Miller et al. (2009) decoded individual finger movements from one hand using electrocorticography (ECoG) [9], suggesting that finer hand movements could be distinguished from electrical signals to generate more control features. Due to the similarity between motor imagery and real movements [10], it provides a promising way to increase DOFs and number of control features produced by MI. However, ECoG is an invasive technique and surgical implantation of ECoG electrodes poses a potential risk for BCI users [11].

In the present study, we investigated the feasibility of discriminating different types of MIs on both hands using the non-invasive scalp EEG through exploring underlying features produced by MIs of thumb and fist from each hand. Variance structures in EEG spectra were analyzed by principal component analysis (PCA) at each channel and a unique spectral structure was identified on which different projections of EEG data from different MIs were suggested. Furthermore, squared cross correlations between each pair of MIs were calculated to identify spatial projection difference of this spectral component between two MIs. The extracted features were then validated using LDA classifiers.

II. Methodology

A. Subjects and Materials

Three subjects volunteered to participate in the study (all males, aged 30 ± 2 and right-handed). Two of them had experience in MI-based BCI, who participated in research of one-dimensional cursor tasks [2]. The third subject was naïve to any BCI paradigms. All of them provided informed consents.

Experiments were conducted in a shielded chamber room under dim light. Subjects were seated in a comfortable armchair with their arms semi-rested. EEG data were recorded using EGI's Geodesic EEG System 300 (GES 300) and a 128-electrode HydroCel Geodesic Sensor Net (HCGSN) (http://www.egi.com). Signals were digitized at 1000 Hz, referenced to an inactive electrode Cz. During recording, subjects were instructed to sit still and avoid movements to reduce motion artifacts. BCI2000, a general-purpose system for BCI research [12], was used to present stimuli to subjects through a LCD monitor. It also streamed EEG data to computers for storage, as well as corresponding event markers

* The work was supported in part by NSF CAREER ECCS-0955260, OCAST HR09-125S, and DOT-FAA10-G-008.

R. Xiao is with the School of Electrical and Computer Engineering, University of Oklahoma, Norman, OK 73019 (corresponding author to provide phone: 4053253774; fax: 4053257066; e-mail: ranxiao@ou.edu).

K. Liao is with the School of Electrical and Computer Engineering, University of Oklahoma, Norman, OK 73019 (e-mail: keliao@ou.edu).

L. Ding is with the School of Electrical and Computer Engineering and Center for Biomedical Engineering, University of Oklahoma, Norman, OK 73019 (e-mail: leiding@ou.edu).

and time stamps. During recordings, no source filters were applied to raw EEG signals.

B. Experimental Design

Stimuli were presented in a sequence of left thumb movement (LTM), MI of left thumb (LT), left fist movement (LFM), MI of left fist (LF), right thumb movement (RTM), MI of right thumb (RT), right fist movement (RFM), MI of right fist (RF), and fixation (Fig. 1). Real-movement cues were included in the design to facilitate subjects' adaption to motor imagination, because two subjects reported having difficulties following MI cues alone during training sessions. Each condition lasted 3 seconds, followed by 2 seconds of blank screen for necessary blinks or swallowing. The whole sequence was repeated 40 times in one session, resulting in 40 trials for each condition and 360 trials in total. In each condition, subjects were instructed to perform either real movements or kinesthetic MI indicated by cues. Trials related to fixations were counted as resting conditions. During this period, subjects sit still and stared at the fixation cross on screen. Only trials related to MIs of thumb and fist and trials from resting conditions were used for subsequent processing. The first subject completed 7 experimental sessions, and other two subjects completed 3 sessions each.

C. Data Preprocessing

EEGLAB [13] was used for preprocessing the acquired EEG data. EEG raw data recorded were first down-sampled to 256 Hz to reduce computational load. Then EEG data from each channel were re-referenced to the common average reference (CAR) obtained across all channels to increase signal-to-noise ratio (SNR) [14]:

$$P_{CAR}(n,t) = P(n,t) - \frac{1}{N}\sum_{i=1}^{N} P(i,t) \cdot \qquad (1)$$

where the common average referenced potential (P_{CAR}) on n_{th} channel was computed by subtracting the recorded potential on n_{th} channel (P) to the average potential across all N channels at each time t.

Bad channels were rejected using Kurtosis method in EEGLAB and interpolated using averaged data from surrounding channels. A band-pass filter (0.03 Hz ~ 70 Hz) and a notch filter (60 Hz) were applied to remove DC offset and reduce influences from power lines. Three-second epoch data corresponding to the length of trials were extracted and categorized according to conditions. Data from trials of four MIs and resting condition were used for subsequent processing.

D. Spectral Principal Component Analysis

Time-series EEG trial data were firstly transferred to frequency domain by calculating power spectrum density (PSD) using Welch's method [15]. Secondly, at each channel, PCA was performed on EEG spectral data pooled from trials related to four MI conditions and resting condition to extract useful spectral features [9]. PCA rotated the original coordinate system to maximize variance of each principal component (PC) in spectra and minimize covariance among PCs [16]. In other words, PCA constructed a rotation matrix,

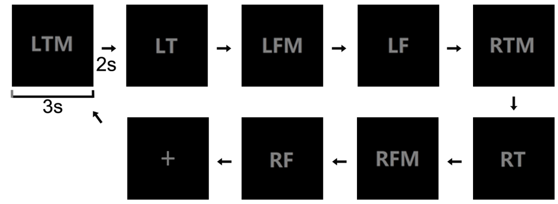

Figure 1. Experimental Design. Each sequence of stimulus starts from LTM and ends with fixation. Each stimulus lasted for 3 seconds and inter-stimulus interval was 2 seconds.

which diagonalized the covariance matrix of original data. In this way, original EEG spectral data were decomposed into various PCs, and spectral features mostly related to all tasks, but indicating difference for different tasks, were identified.

The process of spectral PCA involved multiple steps. Firstly, covariance matrix of EEG spectral data was constructed, revealing inter-frequency correlations and inner-frequency variances produced by trials from all conditions. Secondly, eigenvectors of the covariance matrix were computed, which decomposed EEG spectral data into spectral PCs that reflect spectral features related to MIs. Spectral PCs were sorted by corresponding eigenvalues in a descending order. Finally, EEG spectral data from trials of different MIs were projected onto identified spectral PCs on each channel and their projection weights and associated spatial distributions of these weights were calculated for different MIs.

Only projection weights of the first five PCs were selected for consideration, since they already accounted for the most variation within the EEG spectral data (e.g. 99.97% from Session 1 of Subject 1). Based on projection weights and their spatial patterns, the PC indicating the most distinguishable features among different MIs was identified.

E. Squared Cross Correlation and Classification

Squared Cross correlation (R^2) evaluated the proportion of variance accounted by inter-condition trials to the total variance [17]. It was adopted to reveal spatial difference related to different tasks. Four MI conditions (LT, LF, RT, and RF) in the present study suggested six MI pairs. For each pair, R^2 value was calculated on each channel using data of projection weights of both conditions on the most distinguishable PC. R^2 values from all channels were then mapped onto corresponding channel locations on the scalp. The formula for calculating cross correlation was:

$$R^2 = \frac{(m_1 - m_2)^2}{\sigma_{total}^2} \times \frac{n_1 \times n_2}{n_{total}^2} \cdot \qquad (2)$$

where m_1 and m_2 denoted means of projection weights of two conditions and n_1 and n_2 denoted numbers of trials from each condition. σ_{total}^2 was the group variance and n_{total} was the total number of trials from both conditions. R^2 value was calculated by dividing squared difference of two condition means on group variance. The second term in the equation was to correct unbalanced numbers of trials in two conditions. Channels were rearranged based on their corresponding R^2 values for each MI pair. Only the channels located above cortical areas associated with motor functions and with large R^2 values were selected as feature channels.

In order to evaluate whether identified spatio-spectral features (i.e., spectral PC over feature channels) provided indicative information in decoding different MIs, the linear discriminant analysis (LDA) classifier was used to simultaneously classify four different types of MIs (LT, LF, RT, and RF) using a five-fold cross validation. Eighty percent of trials were used to train LDA classifiers, and the rest were used for test. Each test trial went through six binary LDA classifiers, which were for each pair of conditions. Each LDA classifier voted for one condition and the one with most votes was the final label for the test trial, which was compared to the true label for the calculation of decoding accuracy in each MI. Average accuracy was calculated by averaging decoding accuracies from four MIs. Trials were randomly permuted 50 times for training and testing to yield mean accuracy for each condition. The guess level of four-class problems (i.e., 25%) and its 95% confidence interval (CI) were calculated [18], which served as references for the significance of classification results.

III. Experimental Results

A. PCA Results

Fig. 2(a) presents the average elements (the magnitudes of eigenvectors) of the first five principal components in spectral domain. Results from C3 (on left motor cortex) and C4 (on right motor cortex) were chosen to display since the motor cortex is one of the most important brain areas in MI [10]. Different PCs suggest distinct spectral patterns, revealing different underlying physiological information in spectral domain. Comparing PC elements on C3 and C4, the general structures in the elements of same PCs are similar, while they show variations in magnitudes, especially for the second, third and fifth PCs. The first spectral PC accounts for the largest portion of variance in EEG spectral data [16], which suggests spectral peaks at 12 Hz and 24 Hz of mu and beta rhythms.

Fig. 2(b) visualizes the average projection weights of EEG data from four MIs and resting condition on the first five PCs. The projection weights on the first PC indicate the most

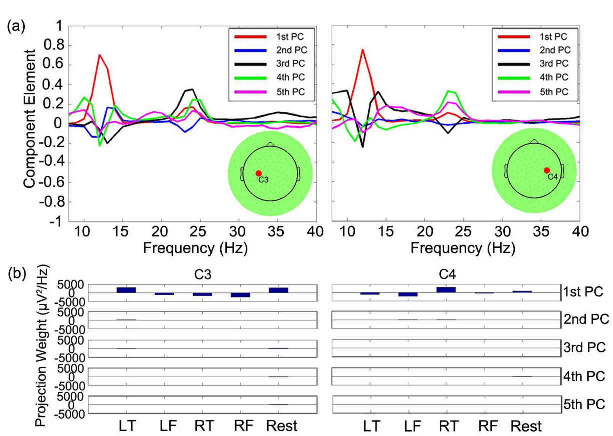

Figure 2. (a) Average elements of the first five PCs from Subject 1; (b) Average projection weights of four MIs and resting condition on the first five PCs from the same subject.

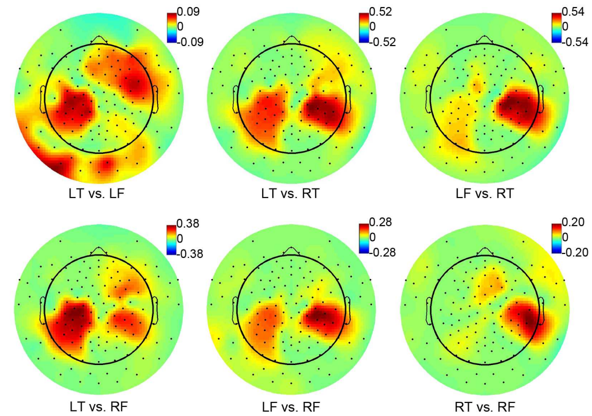

Figure 3. R^2 topographies of six MI pairs from Subject 1. Black dots indicate channel locations. Colorbar represents R^2 values.

distinguishable patterns among different MIs, as well as between MIs and resting condition. While there are some variations on other PCs as well, the difference is relatively small. This might suggest that the most useful information for discriminating different MIs resides in the first PC. Comparing projection weights on the first PC at different channels, it also shows distinct patterns, which indicates distinguishable spectral patterns in different MIs exist in multiple channels. It facilitates the idea to explore spatio-spectral patterns for decoding different MIs.

B. R^2 Topography and Classification Results

Fig. 3 presents the R^2 topographies for each MI pair. It is notable that the magnitudes of R^2 vary across different pairs, with largest R^2 between LF and RT, and smallest R^2 between LT and LF. Most observable differences in spatio-spectral patterns related to the first PC show on the scalp over brain areas related to motor functions in all MI pairs. It further indicates the different spatial patterns among different MI pairs, which suggests distinguishable patterns among four types of MIs.

Fig. 4 shows the classification results for each MI and their average in a four-class MI decoding problem with the use of the identified spatio-spectral pattern. The results show the

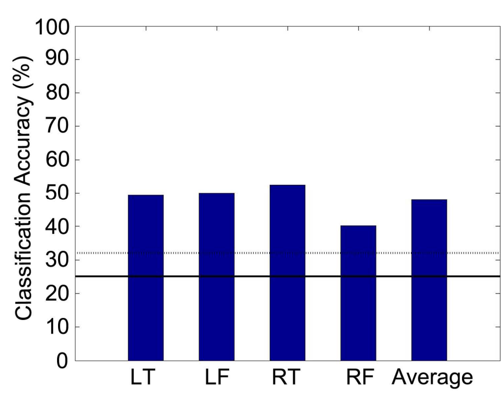

Figure 4. Average decoding accuracy across 3 subjects for each MI type and average decoding accuracy in all trials regardless of conditions. Black solid line indicates 4-class guess level. Dashed line indicates upper boundary of 95% CI of the guess level.

mean decoding accuracies of each condition, obtained from 50 random permutations of all trials. The decoding accuracies vary across different MIs, i.e., LT: 49.4%, LF: 50%, RT: 52.4%, and RF: 40.1%. The decoding accuracies for all conditions are significantly higher than the guess level (25%) and the upper boundary at the 95% CI (32%). The average decoding accuracy reaches up to 48%, which is also significantly higher than the guess level and the upper boundary of 95% CI.

IV. Discussion

In the present study, we explored the underlying spatio-spectral features related to different MIs of thumb and fist on both hands using EEG. PCA and cross correlation analysis were used in extracting corresponding spectral and spatial features, which were further validated by the LDA classifier with 50 times of random permutations. The obtained results (48%) demonstrated the existence of distinguishable features about different MIs of one hand in noninvasive EEG.

Unlike other MI-based BCI studies [1], [2], [19], which only considered MIs from different hands, the present study aims to explore distinguishable features related to MIs of finer movements in one hand, providing a possible mean to increase limited DOFs of control signals for MI-based BCIs. Compared to ECoG-based studies [9], experiments using scalp EEGs are towards a non-invasive BCI, with signals much lower in SNRs and spatial resolutions. Furthermore, data in scalp EEG were from different MI types instead of real movements, which further decreased SNRs in data [10]. These aspects impose difficulties in non-invasive EEG-based BCIs. In addition, MIs from both hands, rather than just from one hand, are included to increase DOFs in the present study. Despite of these difficulties, with the proposed method, extracted spatio-spectral features yield a decoding accuracy significantly higher than the guess level and 95% confidence level when evaluated by simple LDA classifiers.

It is worth to note that extracted features are only on the first PC in this preliminary study. Other PCs can also contain information useful for decoding different MIs. Spatial and spectral features from combination of different PCs may further improve the decoding accuracy. Moreover, since only a simple classifier is used in the present study, more advanced classifiers, such as support vector machine (SVM) classifier [20], can be used to improve decoding accuracy. In addition, MI-based BCIs usually show progressive performance improvements along with training process [2], [4]. More robust features are possible to be extracted, when including more sessions in the future.

In conclusion, we investigated the feasibility of discriminating four different MI types from both hands, with two MIs from the one hand, using non-invasive scalp EEG. With the proposed methods, a spectral component was identified and showed different patterns and spatial distributions in different MIs. Using this new feature, an average decoding accuracy significantly higher than the guess level and 95% confidence level for four types of MIs was achieved when evaluated by a LDA classifier. Our preliminary results demonstrate the potential of a new spatio-spectral feature to generate more control signals for non-invasive BCI applications. In addition, for movement related applications, especially for neuroprosthesis, the present study might facilitate the development of an intuitive BCI paradigm, which depends on users' spontaneous intentions.

References

[1] E. J. X. Costa and E. F. Cabral Jr, "EEG-based discrimination between imagination of left and right hand movements using adaptive gaussian representation," *Med Eng Phys,* vol. 22, pp. 345-348, 2000.

[2] J. R. Wolpaw and D. J. McFarland, "Control of a two-dimensional movement signal by a noninvasive brain-computer interface in humans," *Proc Natl Acad Sci USA,* vol. 101, pp. 17849-17854, 2004.

[3] J. R. Wolpaw, N. Birbaumer, D. J. McFarland, G. Pfurtscheller, and T. M. Vaughan, "Brain–computer interfaces for communication and control," *Clin Nephrol,* vol. 113, pp. 767-791, 2002.

[4] D. J. McFarland, W. A. Sarnacki, T. M. Vaughan, and J. R. Wolpaw, "Brain-computer interface (BCI) operation: signal and noise during early training sessions," *Clin Neurophysiol,* vol. 116, pp. 56-62, 2005.

[5] G. Pfurtscheller, C. Brunner, A. Schlögl, and F. H. Lopes da Silva, "Mu rhythm (de)synchronization and EEG single-trial classification of different motor imagery tasks," *NeuroImage,* vol. 31, pp. 153-159, 2006.

[6] E. W. Sellers, D. J. Krusienski, D. J. McFarland, T. M. Vaughan, and J. R. Wolpaw, "A P300 event-related potential brain–computer interface (BCI): The effects of matrix size and inter stimulus interval on performance," *Biol Psychol,* vol. 73, pp. 242-252, 2006.

[7] B. Z. Allison, D. J. McFarland, G. Schalk, S. D. Zheng, M. M. Jackson, and J. R. Wolpaw, "Towards an independent brain–computer interface using steady state visual evoked potentials," *Clin Neurophysiol,* vol. 119, pp. 399-408, 2008.

[8] D. J. McFarland, W. A. Sarnacki, and J. R. Wolpaw, "Electroencephalographic (EEG) control of three-dimensional movement," *J Neural Eng,* vol. 7, p. 036007, 2010.

[9] K. J. Miller, S. Zanos, E. E. Fetz, M. den Nijs, and J. G. Ojemann, "Decoupling the Cortical Power Spectrum Reveals Real-Time Representation of Individual Finger Movements in Humans," *J Neurosci,* vol. 29, pp. 3132-3137, 2009.

[10] K. J. Miller, G. Schalk, E. E. Fetz, M. Den Nijs, J. G. Ojemann, and R. P. N. Rao, "Cortical activity during motor execution, motor imagery, and imagery-based online feedback," *Proc Natl Acad Sci USA,* vol. 107, pp. 4430-4435, 2010.

[11] A. Presacco, et al., "Towards a non-invasive brain-machine interface system to restore gait function in humans," *Conf Proc IEEE Eng Med Biol Soc*, pp. 4588-4591, 2011.

[12] G. Schalk, D. J. McFarland, T. Hinterberger, N. Birbaumer, and J. R. Wolpaw, "BCI2000: a general-purpose brain-computer interface (BCI) system," *IEEE Trans. Biomed Eng,* vol. 51, pp. 1034-1043, 2004.

[13] A. Delorme and S. Makeig, "EEGLAB: an open source toolbox for analysis of single-trial EEG dynamics including independent component analysis," *J Neurosci Meth,* vol. 134, pp. 9-21, 2004.

[14] D. J. McFarland, L. M. McCane, S. V. David, and J. R. Wolpaw, "Spatial filter selection for EEG-based communication," *Electroen Clin Neuro,* vol. 103, pp. 386-394, 1997.

[15] P. Welch, "The use of fast Fourier transform for the estimation of power spectra: A method based on time averaging over short, modified periodograms," *IEEE Trans. Audio Electroacoust,* vol. 15, pp. 70-73, 1967.

[16] R. A. Johnson and D. W. Wichern, *Applied Multivariate Statisitical Analysis*. Upper Saddle River: Pearson Education Inc, 2007, ch. 8.

[17] P. Shenoy, M. Krauledat, B. Blankertz, R. P. N. Rao, and K.-R. Müller, "Towards adaptive classification for BCI," *J Neural Eng,* vol. 3, p. R13, 2006.

[18] M. D. Mackey and J. L. Melville, "Better than Random? The Chemotype Enrichment Problem," *J Chem Inf Model,* vol. 49, pp. 1154-1162, 2009.

[19] A. S. Royer, *et al.*, "EEG Control of a Virtual Helicopter in 3-Dimensional Space Using Intelligent Control Strategies," *IEEE Trans. Neural Syst Rehabil Eng,* vol. 18, pp. 581-589, 2010.

[20] H. Zhou, Q. Xu, Y. Wang, J. Huang, and J. Wu, "An Improved Support Vector Machine Classifier for EEG-Based Motor Imagery Classification", *Lect Notes Comput Sc*, vol. 5553, pp.267-275, 2009.